Chapter 25
Investigation of Weld Bead Shape Parameters in Relation to Heat Input During Submerged Arc Welding

Satish Kumar Sharma, Dinesh W. Rathod, Himanshu Payal, and Sachin Maheshwari

Abstract In this study, effects of heat input and cooling rate on the weld bead shape-related parameters such as weld penetration shape factor (WPSF) and weld reinforcement form factor (WRFF) are studied during submerged arc welding (SAW) of high strength pipeline steel. Experiments were planned and executed according to the approach of central composite rotatable design (CCRD) using five variables, each at five levels. Along with open circuit voltage, wire feed rate, trolley speed, and contact-tube to work distance, preheating temperature is also used as process variable which governs the cooling rate. For the purpose of prediction as well as better control of weld bead geometry, welding process is mathematically modeled for each weld bead shape-related parameter in relation to process variables. In addition to main and interaction effects, relationship of each weld bead shape-relationship parameter with heat input as well as weld cooling time is presented graphically and further analytically discussed.

Keywords Cooling time · Weld bead · Submerged arc welding · SAW · Heat input · Shape-relationship parameters

25.1 Introduction

For fabrication of oil and gas pipelines, steel grade of high strength such as API X80 is preferred because of its very-fine grain structure possessing high fracture toughness even at low temperatures and also its higher strength-to-weight ratio [1, 2].

S. K. Sharma (✉) · D. W. Rathod
Department of Mechanical Engineering, Thapar Institute of Engineering and Technology, Patiala 147004, India
e-mail: satishsharma847@gmail.com

H. Payal
Department of Mechanical Engineering, Sharda University, Greater Noida 201310, India

S. Maheshwari
Division of Manufacturing Processes and Automation Engineering, Netaji Subhas University of Technology, New Delhi 110078, India

V. S. Sharma et al. (eds.), *Manufacturing Engineering*,
Lecture Notes on Multidisciplinary Industrial Engineering,
https://doi.org/10.1007/978-981-15-4619-8_25

For successful welding of this steel, submerged arc welding (SAW) is the commonly applied welding operation [3]. Geometry of weld bead decides the behavior of welded joint in different applications. However, shape of weld bead is governed by heat input and cooling rate during welding. Therefore, correlation between the welding process parameters and weld bead geometry is important to understand for the better quality of the welds. Due to the involvement of various factors, the relationship between weld bead geometry and welding process parameters is very complex [4–7]. However, control over operating variables in SAW is essential if good quality weld with high production rate is the target [8]. Therefore, in this study, values of weld bead shape-related parameters, weld penetration shape factor (WPSF), and weld reinforcement form factor (WRFF) were calculated. WPSF indicates the internal shape of the weld or centerline cracking possibility in the weld while WRFF indicates the external shape or smoothness of the weld. Table 25.1 summarizes the significance and effect of each weld bead characteristics on the mechanical and microstructure properties possessed by the welded joint.

25.2 Experimentation

25.2.1 Material and Method

High-strength low-alloy pipeline steel is used for bead on plate experiments. Consumables, i.e., electrode filler wire and flux of matching composition, are used according to the AWS specification. Experiments were planned as per CCRD approach of design of experiment, and regression analysis is carried out according to RSM.

25.2.2 Bead Geometry Measurement

Small pieces carrying the complete surface deposited weld bead cross-section and its heat affected zone were taken from 150 mm wide and 300 mm long plate. Figure 25.1 shows the weld deposited cross-sectioned surface after polishing and etching. Bead shape-related parameters were determined using the results of width, penetration, and reinforcement of weld bead measured through stereo-zoom microscope. Table 25.2 lists the process parameters and level values considered during the study. Submerged arc welding process with constant voltage power source is applied in this study.

Table 25.1 Weld bead geometry and its shape-related parameters with significance

Weld bead parameter	Measurement (direct/calculated)	Significance	When at low level	When at high level
Penetration (P)	Direct	Determines the stress-carrying capacity of welded joint	Weak weld joint	May cause centerline cracking
Reinforcement (R)	Direct	Improves the strength of the weld	Less material and lower strength	Excessive material consumption and stress concentration
Bead width (W)	Direct	Indicates the extent of parent material's involvement in welding	Improper fusion of parent material with the filler metal	Tendency for surface cracks. Large area is thermally affected with alterations in its microstructure
Dilution	Calculated as - $\frac{\text{Penetrated Area}}{\text{Total weld Area}}$	Determines the mechanical and chemical properties of a welded joint	A weak joint with lesser penetration	Increases the possibility for solidification cracking in the weld
Reinforcement form factor (WRFF)	Calculated as - $\frac{w}{R}$	Indicates the external shape or smoothness of the weld	Excess material in reinforcement area with non-smooth surface weld	Concave surface of the weld
Penetration shape factor (WPSF) or aspect ratio	Calculated as - $\frac{w}{P}$	Indicates the internal shape of the weld or centerline cracking possibility in the weld	Solidification cracking in the weld	Weld surface tends to crack

25.3 Results and Discussions

25.3.1 Regression Analysis and ANOVA Results

Experiments were carried out at random as given in Table 25.3. From the results of WPSF and WRFF, regression coefficients are determined for a second-order regression model for each weld bead shape-related parameter. ANOVA including tests for the significance of the regression model and coefficients was also performed to check the accuracy of the developed models. Along with goodness of fit test, lack of fit and

Fig. 25.1 For weld number 11, revealed bead geometry after etching

Table 25.2 Process parameters with levels

Process parameters	Notation	Units	Levels				
			−2	−1	0	+1	+2
Open circuit voltage	*A*	Volt	30	32	34	36	38
Trolley speed	*B*	mm/min	250	300	350	400	450
Contact-tube to work distance (CTWD)	*C*	mm	24	28	32	36	40
Preheat temperature	*D*	°C	60	120	180	240	300
Wire feed rate	*E*	mm/s	20	25	30	35	40

model adequacy test were also conducted. ANOVA test results for quadratic model are tabulated in Tables 25.4 and 25.5 for WPSF and WRFF, respectively. Quadratic model for both, WPSF and WRFF is found non-aliased as well as significant. For each model, *p*-value is found <0.0001. Regression model equation for actual values of parameters is given in Eqs. 25.1 and 25.2 for WPSF and WRFF, respectively.

Regression model for actual values of process parameters:

$$\begin{aligned}\text{WPSF} = {} & -85.702 + 4.246 * A + 0.564 * B + 0.701 * C - 0.0404 \\ & * D - 0.086 * E + 1.383\text{E}{-}003 * A * D - 7.08\text{E}{-}003 * B * C - 0.065 \\ & * A^2 - 5.22\text{E}{-}003 * B^2 - 6.66E{-}003 * C^2 - 2.593\text{E}{-}005 * D^2 \end{aligned} \quad (25.1)$$

$$\text{WRFF} = -103.224 + 6.344 * A - 0.1545 * \text{E} - 0.091 * A^2 \quad (25.2)$$

Table 25.3 List of designed experiments with results of WPSF and WRFF

Run No.	*A*	*B*	*C*	*D*	*E*	Critical cooling time $\Delta t_{8/5}$(s)	Heat input (kJ/mm)	WPSF	WRFF
1	1	1	−1	1	−1	16.30	2.48	2.05	2.94
2	0	0	0	0	2	15.74	3.27	1.35	2.08
3	0	0	0	0	0	14.50	3.01	2.29	3.14
4	−1	1	−1	1	1	16.71	2.55	1.19	1.39
5	1	1	−1	1	1	18.15	2.77	1.40	2.24
6	−1	−1	−1	−1	1	12.90	3.49	1.52	2.04
7	0	0	0	0	0	14.35	2.98	2.15	2.79
8	−1	1	−1	−1	−1	8.36	2.26	2.16	3.43
9	0	0	0	0	0	14.37	2.98	2.56	3.92
10	1	−1	−1	1	1	24.37	3.71	1.35	2.18
11	1	−1	1	1	−1	20.86	3.18	2.96	4.56
12	−2	0	0	0	0	11.54	2.40	0.86	1.00
13	0	2	0	0	0	10.25	2.13	1.42	2.28
14	1	1	1	−1	−1	8.67	2.35	2.11	3.65
15	0	−2	0	0	0	18.09	3.76	2.00	2.78
16	0	0	0	0	0	14.35	2.98	2.42	3.60
17	0	0	0	2	0	26.19	2.74	1.41	2.31
18	0	0	0	0	0	14.35	2.98	2.34	3.42
19	−1	1	1	1	−1	14.06	2.14	1.58	2.54
20	1	−1	−1	−1	−1	12.12	3.28	2.42	3.77
21	0	0	0	−2	0	8.16	2.78	2.31	3.08

(continued)

Table 25.3 (continued)

Run No.	*A*	*B*	*C*	*D*	*E*	Critical cooling time $\Delta t_{8/5}$(s)	Heat input (kJ/mm)	WPSF	WRFF
22	1	−1	1	−1	1	10.71	2.90	1.68	2.18
23	−1	−1	1	1	1	20.11	3.06	1.17	1.39
24	0	0	2	0	0	13.10	2.72	2.06	2.24
25	−1	1	1	−1	1	8.82	2.38	1.27	1.36
26	−1	−1	−1	1	−1	19.38	2.95	1.37	1.88
27	0	0	0	0	0	14.35	2.98	2.23	3.30
28	−1	−1	1	−1	−1	10.47	2.83	2.76	3.93
29	0	0	0	0	−2	11.13	2.31	3.21	5.51
30	0	0	−2	0	0	13.36	2.77	1.56	2.74
31	2	0	0	0	0	15.02	3.12	1.53	2.41
32	1	1	−1	−1	1	10.44	2.82	1.30	2.23

Table 25.4 ANOVA results for WPSF

Source	Sum of squares	df	Mean square	*F*-value	*p*-value Prob > *F*	
Model	9.72	11	0.88	25.52	<0.0001	Significant
A-voltage	*0.53*	*1*	*0.53*	*15.21*	*0.0009*	
B-trolly speed	*0.46*	*1*	*0.46*	*13.26*	*0.0016*	
C-CTWD	*0.28*	*1*	*0.28*	*8.04*	*0.0102*	
D-Preheat temperature	*0.66*	*1*	*0.66*	*18.93*	*0.0003*	
E-wire feed rate	*4.39*	*1*	*4.39*	*126.7*	*<0.0001*	
AD	*0.44*	*1*	*0.44*	*12.72*	*0.0019*	
BC	*0.32*	*1*	*0.32*	*9.26*	*0.0064*	
A^2	*2*	*1*	*2*	*57.68*	*<0.0001*	
B^2	*0.5*	*1*	*0.5*	*14.52*	*0.0011*	
C^2	*0.34*	*1*	*0.34*	*9.68*	*0.0055*	
D^2	*0.26*	*1*	*0.26*	*7.43*	*0.013*	
Residual	0.69	20	0.035			
Lack of fit	*0.59*	*15*	*0.039*	*1.87*	*0.2528*	*Not significant*
Pure error	*0.1*	*5*	*0.021*			
Cor total	10.42	31				
Std. dev.	0.19		*R*-squared		0.9335	
Mean	1.88		Adj *R*-squared		0.8969	
C.V. %	9.92		Pred *R*-squared		0.8158	
PRESS	1.92		Adeq precision		21.561	

25.3.2 Main and Interaction Effects

Significance of each regression term is determined at 95% confidence level, and thereafter, using backward elimination, insignificant terms are eliminated. In this section, for each weld bead shape-related parameter, main effects of process parameters are given in terms of perturbation curve, and interaction effects are presented in the form of 3D surface plot.

WPSF: Main effects of SAW process variables on WPSF of the weld can be easily understood by knowing their effects on bead width and penetration, separately. Weld penetration shape factor is found to be affected significantly by all process parameters along with interaction effects of open circuit voltage with preheating temperature and of trolley speed with CTWD. As evident from Fig. 25.2a, WPSF is largely affected by wire feed rate. WPSF decreases almost linearly at very steep rate when wire feed rate is increased. Therefore, more metal deposition rate may be the contributing factor for

Table 25.5 ANOVA results for WRFF

Source	Sum of squares	df	Mean square	*F*-value	*p*-value Prob > *F*	
Model	21.35	3	7.12	22.66	<0.0001	Significant
A-voltage	*3.08*	*1*	*3.08*	*9.81*	*0.004*	
E-wire feed rate	*14.32*	*1*	*14.32*	*45.61*	*<0.0001*	
A^2	*3.95*	*1*	*3.95*	*12.57*	*0.0014*	
Residual	8.79	28	0.31			
Lack of fit	*8.04*	*23*	*0.35*	*2.33*	*0.1758*	*Not significant*
Pure error	*0.75*	*5*	*0.15*			
Cor total	30.14	31				
Std. dev.	0.56		*R*-squared		0.7083	
Mean	2.76		Adj *R*-squared		0.6771	
C.V. %	20.31		Pred *R*-squared		0.6271	
PRESS	11.24		Adeq precision		18.737	

this decrease. Trolley speed and preheating temperature also have a negative impact on WPSF value. Moreover, up to middle levels of open circuit voltage and CTWD, the value of WPSF increases. After that, it decreases with further increase of voltage while remains almost constant with the further increase of CTWD. 3D interaction plot as shown in Fig. 25.2b clearly depicts that higher value of WPSF is given when both preheating temperature and open circuit voltage are kept at their middle level. The interaction between trolley speed and CTWD shown in Fig. 25.2c reveals that higher value of CTWD and lower value of trolley speed are helpful in obtaining a weld with higher WPSF.

WRFF: It is found to be affected significantly by open circuit voltage as well as wire feed rate. As evident from Fig. 25.3, the value of WRFF decreases almost linearly with wire feed rate while it increases when open circuit voltage is increased up to its middle level. With wire feed rate, metal deposition rate also increases which causes higher reinforcement, and hence, a lower value of WRFF is obtained. When voltage is increased, it caused larger increase in bead width as compared to the increase in reinforcement. This change can be a contribution of the increasing arc length. For further increase of voltage, both bead width and reinforcement increase with the almost equal extent, and hence, no significant change in the value of WRFF is obtained.

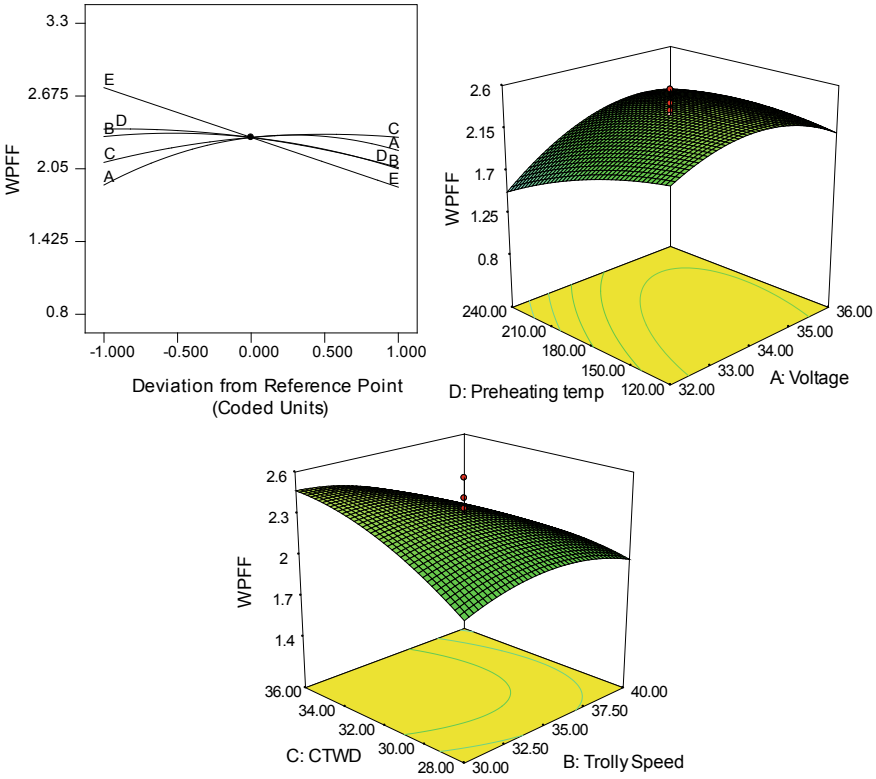

Fig. 25.2 Perturbation curve and interaction effects for WPSF

25.3.3 Relationship Between Bead Shape-Related Parameters and Critical Cooling Time

Critical cooling time ($\Delta t_{8/5}$) is the time period in seconds taken by the weldment to cool down from 800 to 500 °C. Normally, in case of steel, the transformation of its microstructure takes place in this range of temperature. More cooling time indicates the lower cooling rate of the weld with either higher heat input or higher preheating temperature or both. Time taken by the weld to cool down also affects the shape of its bead. In Fig. 25.4, the effect of critical cooling time on each bead geometry characteristic is depicted in the form of graphs. To achieve the desired weld bead shape-related parameters, it is important to understand their relationship with $\Delta t_{8/5}$.

Values of both shape-relationship parameters are decreasing with a slow rate as the $\Delta t_{8/5}$ is increasing as evident from Fig. 25.4. This occurs because bead width is independent of $\Delta t_{8/5}$ while P and R both having an increasing trend with it. This occurs as higher heat input and preheating temperature together yield to a higher cooling time.

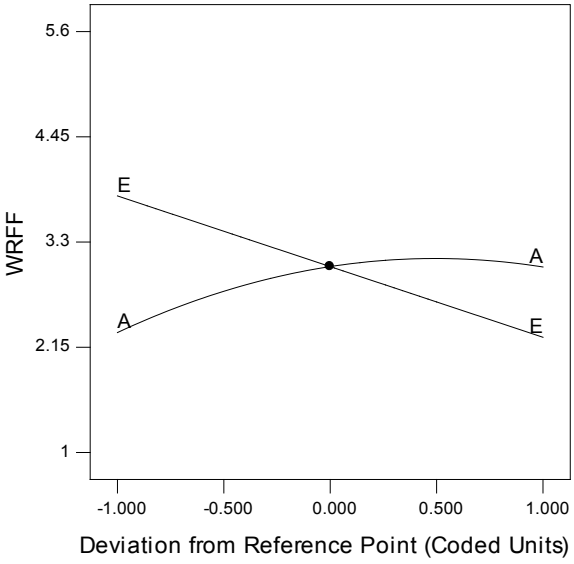

Fig. 25.3 Perturbation curve and interaction effects for WRFF

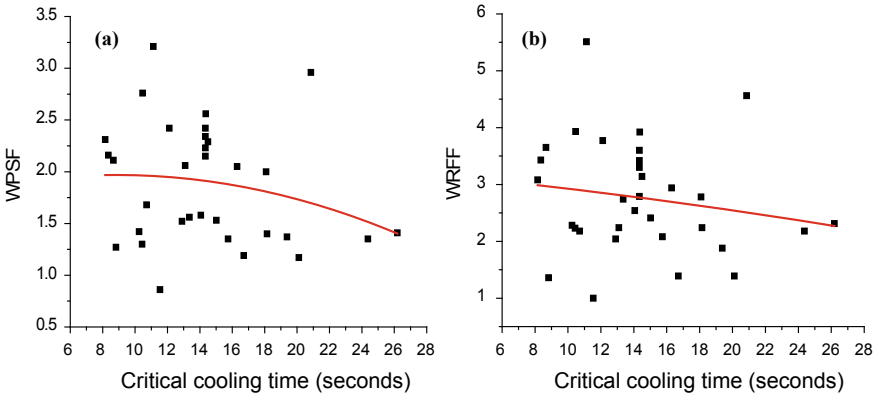

Fig. 25.4 Graph showing variation in **a** WPSF and **b** WRFF; with critical cooling time

25.3.4 Relationship Between Bead Shape-Related Parameters and Heat Input

Because of its higher metal deposition ability, SAW is also a high heat input welding process. Understanding the relation between weld bead shape-related parameters and heat input will help to limit and manage heat input of the process to have better control of the output. Figure 25.5a, b shows that values of bead shape-related parameters increase with heat input of welding. Increase in W and R is mainly because of

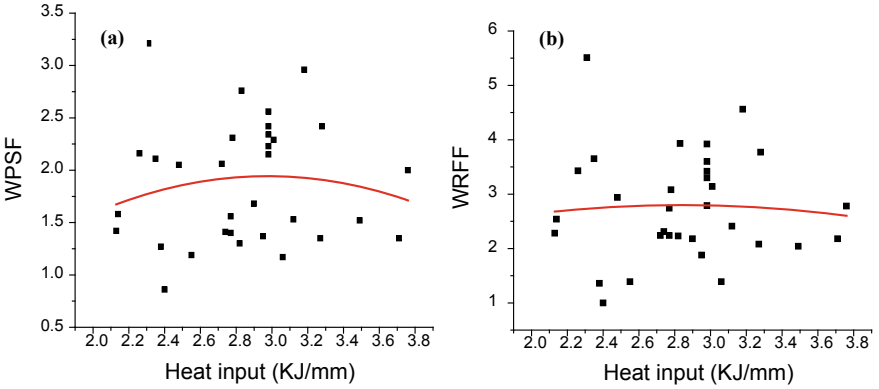

Fig. 25.5 Graph showing variation in **a** WPSF and **b** WRFF; with heat input

the lower trolley speed as well as a dependency of arc length over the voltage and electrode extension. Increased voltage yields to a higher heat input of the process and also increases the arc length as well as the probability for arc blow [9]. Also, voltage affects the dilution of the weld, not its penetration. Similarly, lower trolley speed and higher electrode extension which yields to a higher metal deposition rate as well as heat input in the process result in the increased W and R of the weld. The value of P increases with increase in heat input as with greater heat input, density of current is also high because of higher feed rate of welding electrode. Lower trolley speed with smaller electrode extension gives more concentrated heat to the weldment or plate with negligible arc wandering. This may occur due to increase in both reinforcement and penetration so their corresponding area.

25.4 Conclusions

In this experimental investigation, relationship of weld bead shape-related parameters with heat input of welding process and cooling time of weld is explored during SAW of high strength steel. From the results of the present experimental investigation, following conclusions are drawn:

1. RSM is the suitable approach for regression analysis to provide a quadratic model relating process parameters and process performance measures.
2. Relationship between critical cooling time and bead shape-related parameters provides a clear indication that with increase in critical cooling time, the value of both weld bead shape-related parameters decreases.
3. Up to a certain increase in welding heat input, there is an increase in WPSF due to increase in weld penetration.

4. Results of this study are beneficial for the pipeline industry where welding engineers and pipeline fabricators are more concerned about appropriate weld bead shape-related parameters for sufficient strength of weld and pipeline coating, respectively.

References

1. Felber, S.: Prediction of the mechanical properties and fracture mechanical value of welded joints out of pipeline-steels (X70 and X80). Weld. World. **51**, 14–22 (2007)
2. Sharma, S.K., Maheshwari, S.: A review on welding of high strength oil and gas pipeline steels. J. Nat. Gas Sci. Eng. **38** (2017). https://doi.org/10.1016/j.jngse.2016.12.039
3. Sharma, S.K., Maheshwari, S.: Arc characterization study for submerged arc welding of HSLA (API X80) steel. J. Mech. Sci. Technol. **31** (2017). https://doi.org/10.1007/s12206-017-0238-6
4. Sharma, S.K., Maheshwari, S., Singh, R.K.R.: Modeling and optimization of HAZ characteristics for submerged arc welded high strength pipeline steel. Trans. Indian Inst. Met. **72**, 439–454 (2019). https://doi.org/10.1007/s12666-018-1495-5
5. Sharma, S.K., Maheshwari, S., Rathee, S.: Multi-objective optimization of bead geometry for submerged arc welding of pipeline steel using RSM-fuzzy approach. J. Manuf. Sci. Prod. **16** (2016). https://doi.org/10.1515/jmsp-2016-0009
6. Sharma, S.K., Maheshwari, S., Singh, R.K.R.: Effect of heat-input and cooling-time on bead characteristics in SAW. Mater. Manuf. Process. **34**, 208–215 (2019). https://doi.org/10.1080/10426914.2018.1532578
7. Sharma, S.K., Maheshwari, S.: Multi-objective optimization of HAZ characteristics for submerged arc welding of micro-alloyed high strength pipeline steel using GRA-PCA approach. J. Manuf. Sci. Prod. **16**, 263–271 (2016). https://doi.org/10.1515/jmsp-2016-0027
8. Yin, L., Wang, J., Chen, X., Liu, C., Siddiquee, A.N., Wang, G., Yao, Z.: Microstructures and their distribution within HAZ of X80 pipeline steel welded using hybrid laser-MIG welding. Weld. World. **62**, 721–727 (2018). https://doi.org/10.1007/s40194-018-0582-x
9. Houldcroft, P.T.: Submerged Arc Welding, 2nd edn. Abington Publishing, Cambridge: England (1989)